LIMNOLOGY and OCEANOGRAPHY

ASLO

Limnol. Oceanogr. 9999, 2022, 1–15

doi: 10.1002/lno.12066

Recovery trends of reef carbonate budgets at remote coral atolls 6 years post-bleaching

Ines D. Lange [1*] **Chris T. Perry** [1] **Marleen Stuhr** [2]

[1]Geography, College of Life & Environmental Sciences, University of Exeter, Exeter, UK
[2]Biogeochemistry and Geology, Leibniz Centre for Tropical Marine Research, Bremen, Germany

Abstract

Coral bleaching events and resultant changes in benthic community composition and population size structure can diminish the important geo-ecological functions reefs provide, including habitat provision and carbonate production to support reef accretion. Net reef carbonate budgets, the balance between carbonate production and erosion processes, are thus important functional indicators of reef health. This study quantifies changes in coral community composition and colony size structures, and the resultant reef carbonate budget trajectories after the 2015/2016 bleaching event in the remote Chagos Archipelago, Indian Ocean. *ReefBudget* surveys were conducted at 12 sites across three atolls in 2015, 2018, and 2021, with calculations of biological carbonate production and erosion supported by locally obtained calcification and bioerosion rates. Carbonate budgets (in G = kg $CaCO_3$ m^{-2} yr^{-1}) shifted from net positive states in 2015 (mean ± SD: 3.8 ± 2.6 G) to net negative states in 2018 (−2.4 ± 1.4 G) in response to bleaching-driven mass coral mortality. By 2021, all sites were on a trajectory of recovery, but net budgets differed significantly between atolls (−2.0 ± 1.7 to 2.2 ± 1.4 G). At Salomon atoll, the threefold faster recovery of carbonate production and return to positive reef budget states only 6 yr post-bleaching was associated with the persistence of high structural complexity and the rapid recovery of fast growing tabular *Acropora* spp. Inter-atoll differences in colony size distributions furthermore illustrate that coral identity and size class are more important predictors of reef functions and post-disturbance recovery speed than coral cover alone.

Coral reefs are increasingly impacted by disturbances such as bleaching events, cyclones, and outbreaks of diseases and predators that are becoming more frequent and more severe. These disturbances may either selectively impact coral taxa or lead to large-scale loss of total live coral cover and dramatic alterations to entire reef communities. As a consequence, short- or long-term shifts in community compositions and regime-shifts to fleshy macroalgae have been reported (e.g., McClanahan et al. 2007; Graham et al. 2015). Disturbance events can furthermore alter the size distribution of coral assemblages (Bak and Meesters 1998), either by removing large coral colonies and leaving the remaining assemblage dominated by small corals (McClanahan et al. 2008; Holbrook et al. 2018; Edmunds et al. 2021) or, in contrast, by disproportionally decreasing the relative abundance of small colonies through deficiencies in coral recruitment (Hughes and Tanner 2000; Meesters et al. 2001; Dietzel et al. 2020). Colony size is an important life-history characteristic of corals (Meesters et al. 2001), and there is a growing interest in understanding how changes in individual colony and population dynamics may impact upon the major geo-ecological functions that reefs provide. For instance, changes in the size structure of coral populations, combined with selective taxa losses, may drastically alter the structural complexity of reef environments, which in turn affects fish abundance (Graham et al. 2007; Pratchett et al. 2018). Conversely, a disproportionate abundance of juvenile corals on reefs recovering from disturbances can increase community-level calcium carbonate ($CaCO_3$) production, thereby initially bolstering reef carbonate budgets (Carlot et al. 2021).

In this context, a reef's net carbonate budget reflects the balance between biologically, physically, and chemically

*Correspondence: i.lange@exeter.ac.uk

Additional Supporting Information may be found in the online version of this article.

Author Contribution Statement: IDL led the study, data acquisition and data analysis and wrote the manuscript. CTP contributed substantially to the study's conception, data acquisition and drafting the manuscript. MS contributed to data acquisition and approved the final submitted manuscript.
Special Issue: Cascading, Interactive, and Indirect Effects of Climate Change on Aquatic Communities, Habitats, and Ecosystems.

driven production and erosion processes (Scoffin 1993; Perry et al. 2008) and thereby provides important information on a reef's growth potential and on the capacity of reefs to sustain key geo-ecological functions such as habitat provision and coastal protection (Mace et al. 2014; Brandl et al. 2019). Corals are typically the primary reef framework producers, with additional carbonate being deposited by crustose coralline algae (CCA). On the other side of the budget equation, feeding activities of parrotfish (Bellwood and Choat 1990; Bruggemann et al. 1996) and sea urchins (Bak 1994), and boring activities of endolithic worms, bivalves, and microorganisms (Tribollet and Golubic 2005) erode the reef framework. These biological processes, which largely reflect the abundance of carbonate producing and eroding taxa, are inherently susceptible to ecological disturbances. Indeed, both gradual and steep declines in net carbonate budgets and resultant reef accretion potential have been reported globally due to chronic stress (Perry et al. 2018; Molina-Hernández et al. 2020) and following coral bleaching events (Perry and Morgan 2017; Manzello et al. 2018; Lange and Perry 2019).

While the degradation of coral reefs has been studied extensively in recent decades, critical knowledge gaps remain regarding how rapidly reefs can bounce back and which characteristics enhance reef resilience (Wilson et al. 2010; Graham et al. 2011). Reefs can be resilient to disturbances either by resisting change or by rapidly recovering to their pre-disturbed state (West and Salm 2003; Hodgson et al. 2015). Understanding the processes that drive community recovery is especially critical to predict ecosystem trajectories and manage reefs under increasing global threats (Gouezo et al. 2019). While there are excellent examples of studies that explored recovery trajectories of coral cover and community composition after the global 1997/1998 bleaching event (e.g., McClanahan et al. 2007; Gilmour et al. 2013; Graham et al. 2015), the recovery of reef carbonate budget states is poorly documented. Reef characteristics suggested to speed up ecological recovery are also likely to benefit geo-ecological functions through the maintenance of structural complexity (Connell et al. 1997; Graham et al. 2007; Tanner 2017), high reef connectivity (Ayre and Hughes 2004; Jones et al. 2009; Edmunds et al. 2018), and high levels of herbivory and functional diversity (Mumby et al. 2007; Burkepile and Hay 2008; Adam et al. 2011). Remote reefs that are not exposed to direct human pressures such as pollution and sedimentation from land can serve as model areas to observe natural trajectories of reef recovery after disturbances (Gilmour et al. 2013; Hays et al. 2020).

In this study, we examine temporal trajectories of reef carbonate budget states across the geographically remote northern atolls of the Chagos Archipelago in the central Indian Ocean. These atolls have been exposed to minimal direct or local impacts from fishing, sewage, or shoreline modifications for the last 50 yr (Hays et al. 2020). However, two major global heating events in 1997/1998 and 2015/2016 caused wide-spread coral mortality across the Archipelago and affected reefs to 25 m depth (Sheppard et al. 2017). Most coral reefs recovered to pre-bleaching levels of coral cover and community composition 7–10 yr after the 1997/1998 event (Sheppard et al. 2017), while recovery after 2015/2016 is currently ongoing. In order to examine temporal and spatial patterns of reef carbonate budget states, we quantified benthic communities and bioeroder populations on fore-reef sites across three atolls in 2015, 2018, and 2021 using the *ReefBudget* methodology. We then explore the reasons why rates of recovery have differed between the atoll locations. Our analysis provides important insights into trajectories of geo-ecological reef functions after a bleaching event, and thus assists in understanding the ecological factors influencing recovery rates in the absence of local stressors.

Materials and methods

Study sites

The Chagos Archipelago is part of the Lakshadweep-Maldives-Chagos ridge in the central Indian Ocean and consists of five atolls with islands, and numerous submerged banks (Fig. 1). While local impacts are minimal due to the remoteness and protected status of the area (apart from continued impacts of

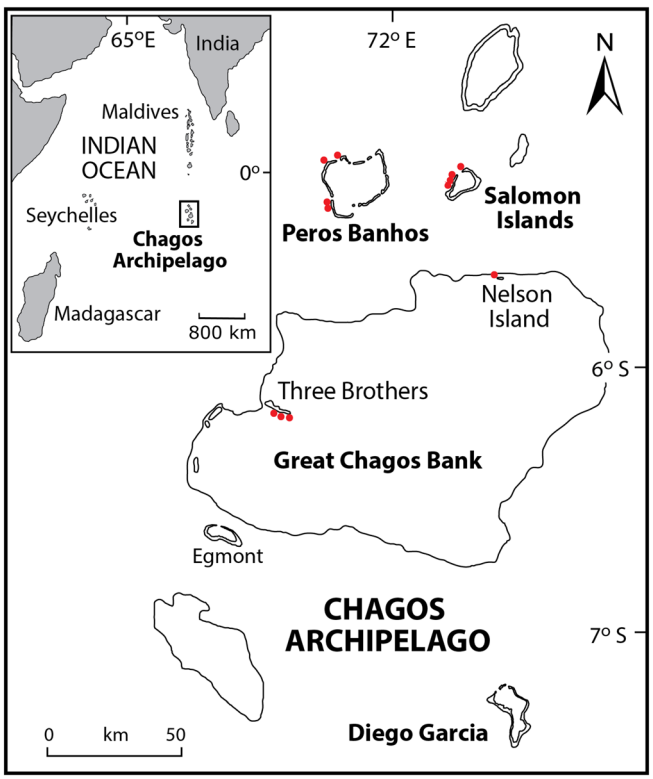

Fig. 1. Map of study sites (red symbols) across the northern atolls of the remote Chagos Archipelago, central Indian Ocean.

illegal fishing), its coral reefs were severely impacted by the most recent global bleaching event in 2015/2016 (Hays et al. 2020). Pre-bleaching (April 2015), most fore-reefs across the Chagos Archipelago had high coral cover (averaging 40%–50%; Sheppard et al. (2017)) and high net positive carbonate budgets (up to 9.8 kg $CaCO_3$ m^{-2} yr^{-1}; Perry et al. (2015*a*)). Widespread coral bleaching and mortality in 2015 and 2016 reduced hard coral cover to <10% at 5–20 m depths (Sheppard et al. 2017), with severe implications for coral carbonate production rates, which decreased by 77% (Lange and Perry 2019). The latter study did not determine full net reef budgets as erosion rate data were unavailable, and estimations of carbonate budgets in both 2015 and 2018 relied on published rates of calcification and bioerosion from across the wider Indo-Pacific, as no local rate data existed.

In order to more accurately quantify the decline and, more importantly, the early recovery of net reef carbonate budgets in response to the 2015/2016 bleaching event, we re-analyzed data from March to April 2015 and May 2018 using newly available local data on coral growth rates, skeletal densities, crustose coralline algae (CCA) calcification rates, and parrotfish bioerosion (detailed below). We then compared the results to data from the same 12 fore-reef sites across the atolls of Salomon (SA), Peros Banhos (PB), and Great Chagos Bank (GCB) (n = 4 sites/atoll, Fig. 1) collected in April–May 2021, 6 yr after the bleaching event. Surveyed fore-reefs across all atolls were characterized by a gently sloping reef terrace in 8–10 m depth before dropping-off to >25 m depth. All sites were defined as sheltered from predominant wind direction and wave exposure (south-easterly), except reefs at Middle and South Brother (GCB), which are located along the moderately exposed south coasts of these islands (Perry et al. 2015*a*). Water temperatures at fore reefs across the Archipelago average 27–29°C, with short-term plunges of 5–7°C between February and April caused by tidal and internal waves (Sheppard 2009).

ReefBudget methodology

Gross carbonate production, gross carbonate erosion, and net reef carbonate budgets were estimated using the Indo-Pacific *ReefBudget* methodology (available at https://geography.exeter.ac.uk/reefbudget/). At each site, data were collected along four replicate transects (10 m long) placed on the reef terrace along a depth contour in 8–10 m depth. For substrate composition, we measured the distance (in cm) covered by each benthic group beneath the 10 m guide transect line using a separate flexible tape and following the reef contour. Recorded groups included scleractinian corals to the genera and morphological level, for example, *Acropora* tabular, *Porites* massive etc.; crustose coralline algae (CCA); turf algae; fleshy macroalgae; non-encrusting coralline algae (e.g., *Halimeda* spp.); sediment; rubble; sponges; and other benthic organisms. Distances of benthic categories were collected as a function of the true three-dimensional (3D) surface of the reefs, including cover on overhangs and vertical surfaces, and thus exceed linear transect length. The cumulative total reef surface was divided by linear distance (10 m) to yield rugosity, a measure for structural complexity of the reef substrate (Risk 1972). Survey data were entered into the *ReefBudget* spreadsheets, which use the morphology and size of individual coral colonies in combination with genera/morphotype-specific calcification rates to estimate total annual coral carbonate production (Coral G with G = kg $CaCO_3$ m^{-2} yr^{-1}). Cover of CCA was multiplied by an average local calcification rate to estimate CCA carbonate production (CCA G) and was added to Coral G to yield Gross Production G. Endolithic bioerosion by macroborers (e.g., sponges, polychaetes, bivalves) and microborers (e.g., algae, fungi) were taken into account by multiplying published bioerosion rates with the available substrate along each transect (all benthic categories except sand) to yield annual endolithic erosion (Macro G and Micro G). Sea urchin abundance and test-size was determined in belt transects along the same four transects (10 × 2 m) and their contribution to erosion calculated using published taxa- and size-specific erosion rates (Urchin G). Parrotfish abundance and size (to nearest cm) was quantified along four separate transects (50 × 5 m). In 2021, parrotfish surveys at each site were conducted the same day as benthic surveys. For the calculation of budget states in 2015 and 2018, parrotfish data were extracted from fish surveys conducted in 2010 and 2019, respectively, at the same sites and using the same method as in 2021 (n = 4, 50 × 5 m, size to nearest cm) (data collected by NAJ Graham and reported in Lange et al. 2020). The only exception were three sites (Nelson [GCB], Ile du Passe [PB], Ile de la Passe [SA]) that were surveyed along eight transects (30 × 5 m) in 2015, with observed parrotfish grouped into 10 cm size classes. For sites without any survey data (n = 3 in 2010 and n = 4 in 2019), parrotfish data from the same year and nearest site were used instead (*see* data table at https://doi.org/10.24378/exe.3863). Bioerosion for each observed parrotfish was calculated using species- and size-specific erosion rate data and averaged across transects to yield site-specific annual erosion by fish (Parrotfish G). Erosion by each functional group was summed at transect-level, except fish erosion, which was determined along separate transects and was therefore factored in as an average value, to yield Gross Erosion G, which was subtracted from Gross Production G to yield the net carbonate budget (Net G).

Local calcification and bioerosion rates

To provide the most accurate carbonate budget estimates possible, considerable effort was invested in collecting local and current datasets on taxa-specific calcification and erosion rates (available at https://doi.org/10.24378/exe.3863). These rates represent the first estimates available for the region and were used for the calculation of carbonate budgets across the 6-yr study period.

Coral calcification rates were calculated from measured colony sizes (cm), linear growth rates (cm yr^{-1}), skeletal densities (g cm^{-3}) and, in the case of branching taxa, conversion factors to take into account the ratio of growing branch tips to total colony size. The conversion factors were determined by measuring the size of branching colonies and the length of growing tips across 337 colonies of different Indian Ocean coral genera, and are reported in the *ReefBudget* handbook. Local linear growth rates were determined for 64 individual coral colonies (size 12–50 cm diameter) of the dominant 22 genera-morphotypes (n = 1–7 colonies/type) on two of the surveyed fore reef sites (Ile Poule, PB, Middle Brother, GCB) in 8–10 m depth, by comparing 3D models of the same coral colonies in 2018 and 2019. Models were constructed from underwater photographs using the Structure-from-Motion software Agisoft Metashape Professional (version 1.5.1) following the protocol described in Lange and Perry (2020). The precision of model building using this method is ≤ 0.2 mm, and standard deviation of growth measurements is ≤ 0.9 mm. The measured growth rates in 2018/2019 can be considered conservative estimates for 2015 and 2021, as some species might have shown decreased calcification after the heat stress event (Manzello et al. 2018; Leupold et al. 2019). However, the repeated assessment of a subset of these colonies (n = 17) in 2021 did not show significantly different annual growth rates in the period 2019–2021 compared to 2018–2019 (*t*-tests, ns).

Skeletal densities were determined for 136 individual coral colonies (n = 5 fragments/colony) of 35 genera-morphotypes, which were collected from fore reefs in 8–10 m depth across the Chagos Archipelago in 2019. Fragments were sprayed with a water hose to remove all tissue, soaked in sodium hypochlorite solution overnight and dried in the sun for transport. Before analysis, fragments were again dried at 40°C for 15 h. Bulk density of coral fragments was acquired using the Archimedes principle after Bucher et al. (1998). After obtaining the dry weight of clean coral skeleton (DW_{clean}), a thin coating of paraffin wax (Paraplast X-TRA®) was applied to each piece of coral by quickly dipping it into a pot of molten wax (in water bath at 74–79°C) and shaking off the excess. Waxed skeleton fragments were allowed to cool for a few minutes before being weighed dry (DW_{wax}) and suspended in water (BW_{wax}). The density of the water (ρ_{water}) in the aquarium below the scale was determined every 10 fragments by weighing a stainless steel cube of known density (7.91 g cm^{-3}). Bulk density of each coral skeleton fragment (ρ_{coral}) was calculated as follows and averaged to yield colony skeletal density:

$$\rho_{coral}\left(\mathrm{g\,cm^{-3}}\right) = \frac{DW_{clean}}{DW_{wax} - BW_{wax}} \times \rho_{water}$$

$$\text{with } \rho_{water}\left(\mathrm{g\,cm^{-3}}\right) = 7.91 \times (1 - (BW_{cube} - DW_{cube}))$$

Average CCA calcification was obtained by deploying lightly sanded PVC cards (8.5 × 5.4 cm) on fore reefs in Salomon atoll and Great Chagos Bank (n = 10/site) in 8–10 m depth for 1 yr (2018–2019). Cards were attached to PVC pipes and deployed in both horizontal and vertical orientation, although orientation did not result in distinct encruster communities or calcification rates (*t*-tests, ns) and thus average rates across all deployed tiles were used. Recovered tiles, which were all covered in thick CCA crusts, were bleached overnight, dried for 24 h in a drying oven at 60°C for transport and again dried at 40°C for 48 h before analysis. The dried PVC cards and any loose material were weighed on a precision analytical balance (PVC_{crust}), before all $CaCO_3$ that accumulated on the cards was dissolved by gradually adding ca. 80 mL 10% HCl per sample over 30–60 min and again after a few hours until no new bubbles formed. PVC cards and the remaining loose organic material, which was filtered through pre-weighed Whatman 1 filters ($filter_{empty}$), were rinsed with distilled water, dried at 40°C for 24 h and reweighed (PVC_{empty} and $filter_{org}$). Annual calcification was then calculated as follows:

$$\text{CCA calcification}\left(\mathrm{g\,cm^{-2}\,yr^{-1}}\right) = \frac{PVC_{crust} - PVC_{empty} - \left(filter_{org} - filter_{empty}\right)}{\text{Area}} \times \frac{365}{\text{Days of exposure}}$$

Average CCA calcification across the two sites was 0.057 ± 0.011 g cm^{-2} yr^{-1} (mean ± SD). Similar protocols to determine CCA calcification have been used in other studies, and yielded similar rates for the Maldives (0.045 ± 0.019 g cm^{-2} yr^{-1}; Morgan and Kench (2014)) and across all available studies in the Indo-Pacific with deployment time ≥ 1 yr (0.040 ± 0.019 g cm^{-2} yr^{-1}, IP calcification database v1.3 at https://geography.exeter.ac.uk/reefbudget/, accessed 15 December 2021).

Bioerosion rates for the dominant three excavating (*Cetoscarus ocellatus, Chlorurus strongylocephalus, Chlorurus sordidus*) and six scraping parrotfish species (*Scarus rubroviolaceus, Scarus frenatus, Scarus tricolor, Scarus niger, Scarus scaber, Scarus psittacus*) were modeled from species- and size-specific feeding metrics quantified in the Chagos Archipelago and the southern Maldives in 2019 and 2020, with details provided in Lange et al. (2020). In short, allometric relationships between bite rates (*bpm*), proportion of bites leaving scars (*% scars*), or bite volumes (*vol*) with body length were used to calculate bioerosion rates for each individual fish of a certain size (in cm) or size class (midpoint of size class) as follows:

$$\text{Bioerosion}\left(\mathrm{kg\,ind^{-1}\,year^{-1}}\right) = vol \times \frac{\text{Density}}{10^3} \times \%scars \times bpm \times 60 \times \text{daylight} \times \text{proportion feeding} \times 365$$

An average substrate density of 1.52 ± 0.19 g cm^{-3} was used, which is the mean (± SD) bulk density of all coral

density samples described above (range: 1.03–1.98 g cm^{-3}). As the study sites are located very close to the equator, 12 h of daylight was used for calculations. Proportion of day feeding was adapted from Bellwood et al. (1995): 83.3% for large parrotfish (*C. ocellatus, Ch. strongylocephalus, S. rubroviolaceus*) and 87.7% for smaller species (*Ch. sordidus* and other *Scarus* spp.).

Community composition

The *ReefBudget* result sheet summarizes percent cover of individual taxa and benthic categories to yield average site-level cover of total live coral, CCA, turf, sponges, soft corals, macroalgae, rubble, sand, and others. Furthermore, the relative contribution of each genera/morphotype to total coral cover is reported for tabular *Acropora*, other *Acropora* (corymbose, digitate, and open branching), *Pocillopora*, branching *Porites*, other branching corals, massive *Porites*, other massive corals, encrusting *Porites*, other encrusting corals, foliose corals, free-living corals, and others. Both the main categories and the taxa contribution to total coral cover were used for analyses of benthic community composition and coral community composition, respectively.

Coral colony size structure

Coral colony sizes for all coral colonies, tabular *Acropora*, other *Acropora* (mainly corymbose and digitate, few open branching), branching (*Pocillopora*, *Stylophora*, other taxa except *Acropora*), massive (mainly *Porites* but also all other taxa), and encrusting (all taxa) morphologies were extracted from benthic datasets to examine changes in the size structure of entire communities and individual groups across atolls and over time. Columnar, foliose, and free-living morphologies occurred rarely and were therefore not analyzed individually. Due to the nature of *ReefBudget* data collection, colony sizes represent colony contour lengths, rather than planar colony area or diameter used in other studies (Meesters et al. 2001; Riegl et al. 2012; Dietzel et al. 2020), and depict lengths of continuous live coral tissue cover (as in McClanahan et al. 2008) and not estimates of total colony size connected by a shared skeleton (as in Dietzel et al. 2020). An increase in the abundance of small colonies can therefore indicate recruitment and/or fragmentation of larger massive or encrusting colonies through partial mortality. A total of 4099 colony sizes were recorded across all morphotypes, years and sites.

Statistics

All statistical analysis was conducted in R v4.1.0 (R Core Team 2021) using packages *vegan* (Oksanen et al. 2020) and *tidyverse* (Wickham et al. 2019).

Coral cover and carbonate budgets

Spatial and temporal differences in coral cover, substrate rugosity, gross carbonate production, gross carbonate erosion, and net budgets were examined using two-way ANOVA (2-way ANOVA) with fixed factors *atoll* and *year*, followed by Tukey multiple pairwise-comparison to determine which specific pairs differed significantly. Interactions between *atoll* and *year* were not significant and are therefore not reported in the text. Assumptions of homogeneity of variances and normality were confirmed via visual observation of residual plots and using Levene and Shapiro–Wilk tests. Statistical outputs of two-way ANOVAs and Tukey post-hoc tests are provided in Supplementary Table S1.

Community composition

To examine differences in overall benthic community structure, we used non-metric multidimensional scaling (NMDS) on Bray–Curtis similarity matrices for (1) proportional cover of benthic categories and (2) proportional contribution of coral taxa to total live coral cover following analyses detailed in Benkwitt et al. (2019). We conducted PERMANOVAs to test for differences between atolls and years and their interaction (Anderson and Walsh 2013) and used SIMPER analysis to determine which organisms drove dissimilarities between communities that were significantly different from each other (Clarke 1993). Multivariate homogeneity of group dispersion was tested using the PERMDISP2 procedure (Anderson 2005) and indicated that centroids did indeed vary in multivariate space and not due to within-atoll variability. Statistical outputs of NMDS, PERMANOVA, PERMDISP2, and SIMPER procedures are provided in Supplementary Table S2.

Coral colony size structure

Trends in colony size structure over time were examined graphically from size-frequency distributions and as changes in size-class abundances following analyses detailed in Dietzel et al. (2020). In short, colony size data were log-transformed and binned into small (first quintile), medium (second to fourth quintile), and large (fifth quintile) colonies using bootstrap resampling ($n = 1000$) to assess uncertainties in size-class abundances. Size classes were calculated for each morphotype individually, but pooled across atolls and years. Additionally, mean size and standard deviation (SD) of all colonies and skewness of size frequency distribution at each atoll and year were compared using non-parametric Kruskal–Wallis tests (to account for non-normally distributed distribution parameters), followed by Dunn's post-hoc comparisons with Holm's adjustment of *p*-values. Statistical outputs are provided in Supplementary Table S3.

Results

Coral cover, substrate rugosity, and community composition

Mass coral mortality during the 2015/2016 bleaching event decreased average live coral cover on fore reefs across the Chagos Archipelago from (mean ± SD) 27.4 ± 10.5% in 2015 to 8.5 ± 3.9% in 2018 (Fig. 2A, Table 1). This trajectory was accompanied by declines in average substrate rugosity from 2.3 ± 0.2 in 2015 to 1.9 ± 0.3 in 2018 (Fig. 2B). While coral

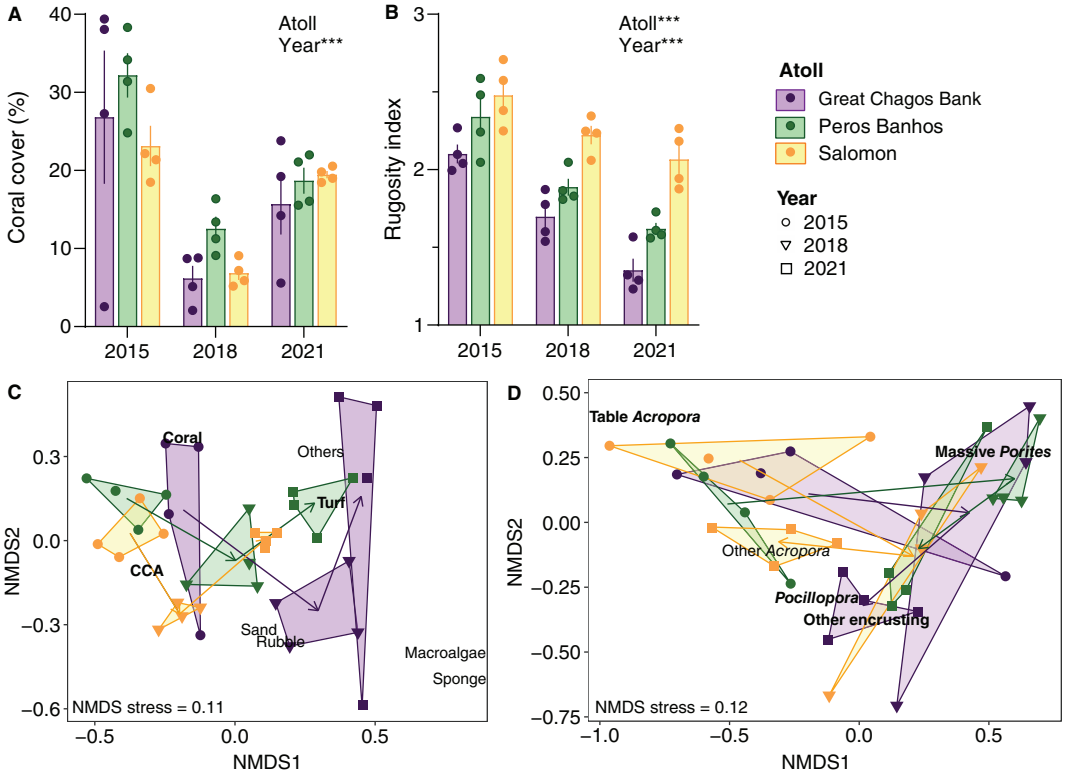

Fig. 2. Changes in reef communities across the Chagos Archipelago in response to the 2015/2016 bleaching event. The first row shows spatial and temporal patterns in (**A**) coral cover and (**B**) substrate rugosity. Points represent site-level data and bar plots indicate mean ± SE at each atoll (color). Results from two-way ANOVAs are indicated by significance levels in the upper right corner (*< 0.05, **< 0.01, ***< 0.001), full ANOVA tables with Tukey post-hoc results are provided in Supplementary Table S1. The second row depicts non-metric dimensional scaling (NMDS) plots of (**C**) benthic communities and (**D**) coral communities across atolls (color) and years (symbols). Each point represents a site in species space, with the distances among points approximating dissimilarities among communities. Shaded areas represent minimum convex hull polygons, and arrows show movement of centroids through time. Only species that contributed significantly to the dissimilarity among sites or years (based on envfit analysis) are displayed on the plot and labels in bold represent the primary drivers of dissimilarities among communities (based on SIMPER analysis).

Table 1. Average coral cover, rugosity, and carbonate budget states across atolls and time. All values are stated as mean ± standard deviation ($n = 4$ sites/atoll). Carbonate production and erosion rates of each major group are presented in G = kg $CaCO_3$ m^{-2} yr^{-1}.

	Great Chagos Bank			Peros Banhos			Salomon		
	2015	**2018**	**2021**	**2015**	**2018**	**2021**	**2015**	**2018**	**2021**
Coral cover (%)	26.8 ± 17.1	6.2 ± 3.2	15.7 ± 7.8	32.2 ± 5.7	12.5 ± 3.1	18.7 ± 3.3	23.1 ± 5.2	6.8 ± 1.7	19.5 ± 0.9
Rugosity	2.1 ± 0.1	1.7 ± 0.2	1.4 ± 0.1	2.3 ± 0.2	1.9 ± 0.1	1.6 ± 0.1	2.5 ± 0.2	2.2 ± 0.1	2.1 ± 0.2
Coral G	6.4 ± 3.8	1.3 ± 0.6	2.4 ± 0.7	7.8 ± 1.1	2.6 ± 0.4	3.6 ± 0.7	6.7 ± 1.2	1.9 ± 0.5	5.6 ± 0.3
CCA G	0.5 ± 0.2	0.3 ± 0.1	0.1 ± 0.0	0.6 ± 0.1	0.5 ± 0.1	0.2 ± 0.0	0.7 ± 0.2	0.8 ± 0.1	0.3 ± 0.0
Macro G	−0.4 ± 0.1	−0.3 ± 0.0	−0.3 ± 0.0	−0.4 ± 0.0	−0.4 ± 0.0	−0.3 ± 0.0	−0.5 ± 0.1	−0.4 ± 0.1	−0.4 ± 0.0
Micro G	−0.5 ± 0.0	−0.4 ± 0.0	−0.3 ± 0.0	−0.6 ± 0.1	−0.5 ± 0.0	−0.4 ± 0.0	−0.6 ± 0.1	−0.6 ± 0.0	−0.5 ± 0.0
Urchin G	−0.9 ± 0.9	−1.6 ± 1.2	−1.0 ± 0.9	−0.0 ± 0.0	−0.0 ± 0.0	−0.0 ± 0.0	−0.0 ± 0.0	−0.0 ± 0.0	−0.0 ± 0.0
Fish G	−2.6 ± 0.8	−3.0 ± 0.4	−3.0 ± 1.3	−3.5 ± 1.9	−4.5 ± 1.0	−4.4 ± 1.7	−1.4 ± 1.8	−2.9 ± 0.1	−2.8 ± 1.4
Gross Product. G	6.8 ± 3.6	1.6 ± 0.6	2.5 ± 0.8	8.4 ± 1.2	3.1 ± 0.4	3.8 ± 0.7	7.5 ± 1.1	2.6 ± 0.5	5.9 ± 0.3
Gross Erosion G	−4.4 ± 0.7	−5.3 ± 1.2	−4.5 ± 1.2	−4.5 ± 1.8	−5.3 ± 1.1	−5.1 ± 1.7	−2.5 ± 1.7	−3.9 ± 0.1	−3.7 ± 1.4
Net Budget G	2.4 ± 3.9	−3.7 ± 1.1	−2.0 ± 1.7	3.9 ± 2.3	−2.3 ± 1.4	−1.3 ± 1.2	5.0 ± 0.9	−1.3 ± 0.4	2.2 ± 1.4

cover recovered to 17.9 ± 4.8% over the next 3 yr (recovery rate GCB: 3.2% yr^{-1}, PB: 2.0% yr^{-1}, SA: 4.2% yr^{-1}), rugosity continued to decrease to 1.7 ± 0.1 in 2021, with faster degradation rates in Great Chagos Bank and Peros Banhos compared to Salomon (−5.9%, −5.1%, and −2.9% yr^{-1}, respectively). Relative live coral cover thus differed significantly between all years (ANOVA, *year*: $F = 21.55$, $p < 0.001$; Supplementary Table S1), but not between atolls, while substrate rugosity differed between all years and atolls (*year*: $F = 47.25$, $p < 0.001$; *atoll*: $F = 34.75$, $p < 0.001$; Supplementary Table S1).

Benthic community composition also differed significantly on spatial and temporal scales. Reef communities were similar across all atolls in 2015 (Fig. 2C), apart from one outlier site in Great Chagos Bank that had been severely impacted by a crown-of-thorns outbreak in 2013 and therefore already had low coral cover in 2015. After the bleaching event, all sites shifted toward communities characterized by higher cover of CCA, turf, sand, and rubble, but compositions became more distinct across atolls by 2021. Statistical analysis of this data shows that the impact of bleaching and recovery was stronger than that of location, and that temporal and spatial factors were independent from each other (PERMANOVA, *year*: $F = 20.46$, $p = 0.001$, *atoll*: $F = 5.62$, $p = 0.001$, *year*atoll*: $F = 1.44$, $p = 0.181$; Supplementary Table S2). The primary driver of differences between 2015 and 2018 was coral cover, explaining 11.3% of the dissimilarity between sites, while differences between 2018 and 2021 were mainly driven by CCA cover, explaining 9.8% of dissimilarity (SIMPER, $p = 0.001$ and 0.015, respectively; Supplementary Table S2). Differences between 2015 and 2021 were mainly due to CCA and turf, explaining 13.1% and 9.7% of the dissimilarity, respectively (both $p = 0.001$). Differences between atolls were mainly driven by cover of coral (GCB vs. PB: 7.8%, $p = 0.040$) and CCA (GCB vs. SA: 10.0%, $p = 0.009$), with Peros Banhos and Salomon showing no significant differences in community composition across years.

In terms of the relative abundance of coral taxa (Fig. 2D), tabular *Acropora* spp. dominated live coral cover in all atolls in 2015 (32.6 ± 18.3%), but communities shifted to a relative dominance of massive *Porites* spp. and encrusting taxa in 2018 (45.6 ± 21.1% and 32.1 ± 17.4%, respectively) and 2021 (19.4 ± 11.4% and 30.8 ± 7.1%, respectively). Differences between atolls were less pronounced, apart from the relative contribution of tabular *Acropora* spp. to total coral cover, which across all years was higher at Salomon (20.8 ± 21.1%) compared to Peros Banhos (12.1 ± 18.4%) and Great Chagos Bank (8.4 ± 15.0%), mainly due to cover differences in 2021 (4.5 ± 2.4% of substrate cover compared to 0.4 ± 0.4% and 0.2 ± 0.2%, respectively). This illustrates that, again, the effect of year was higher than that of atoll in structuring coral communities (PERMANOVA, *year*: $F = 13.37$, $p = 0.001$, *atoll*: $F = 3.13$, $p = 0.008$, *year*atoll*: $F = 1.24$, $p = 0.269$; Supplementary Table S2), but it also shows that the return toward pre-bleaching status is much further progressed at Salomon compared to the other two atolls (Fig. 2D).

Coral colony size structure

Bleaching-induced changes in benthic communities were not only visible as declines in coral cover and shifts in community composition, but also in changing coral population size structures. Total abundance of coral colonies declined sharply from 2015 ($n = 1426$) to 2018 ($n = 880$) across all atolls and morphotypes. Declines were especially pronounced for tabular *Acropora*, which disappeared completely in 2018, as well as for other *Acropora* and branching corals, which also suffered high whole coral colony mortality rates (Fig. 3A). Massive and encrusting morphotypes experienced a loss of larger colonies accompanied by an increase in the number of smaller colonies (Fig. 3A), which was likely largely caused by partial mortality of colonies resulting in several smaller patches of live tissue. Overall, mean colony size declined significantly from 22 ± 24 cm in 2015 to 11 ± 13 cm in 2018 (Fig. 3B, Kruskal–Wallis: $\chi^2 = 17.97$, $p < 0.001$; Supplementary Table S3). Standard deviation of colony size and skewness of size distributions also decreased significantly following bleaching (SD Kruskal–Wallis: $\chi^2 = 18.25$, $p < 0.001$; skewness Kruskal–Wallis: $\chi^2 = 7.44$, $p < 0.024$; Supplementary Table S3), independent of site location (Fig. 3B). The overall positive skewness indicates that coral populations were generally dominated by small colonies, with lower skewness in 2018 when large colonies disappeared, and the right tails of the frequency distributions therefore shortened. Indeed, the abundance of large colonies (i.e., colonies within the fifth quintile of group-specific size distributions) declined by 76% in Great Chagos Bank, 71% in Peros Banhos, and 66% in Salomon (Fig. 4). Especially evident was the complete loss of large tabular *Acropora* spp. colonies, of which 11% measured ≥100 cm in 2015 (maximum size 243 cm).

Over the following 3 yr, total colony abundance increased to above pre-bleaching levels ($n = 1793$), critically including high numbers of *Acropora* spp. juveniles (Fig. 3A), but mean colony size by 2021 remained small (10 ± 11 cm, Fig. 3B), due to increasing abundances of small colonies and the continued lack of large table corals. Only 5% of tabular *Acropora* colonies measured >50 cm in 2021 (maximum size 67 cm). Differences in recovery patterns between atolls are visible in terms of dominant taxa, colony abundances and size frequency distributions. While total abundance of coral colonies and skewness of size distributions increased rapidly at both Peros Banhos and Salomon, this was partly driven by increases in tabular *Acropora* spp. at Salomon, but by massive and encrusting colonies at Peros Banhos (Fig. 3A). Increases in abundance were mainly detected in the small colony size class in all atolls, indicating new coral recruitment from 2018 to 2021 across all morphotypes. At the same time, growth of remaining corals pushed the size distribution curves to the right. This was especially visible for *Acropora* spp. and branching morphotypes,

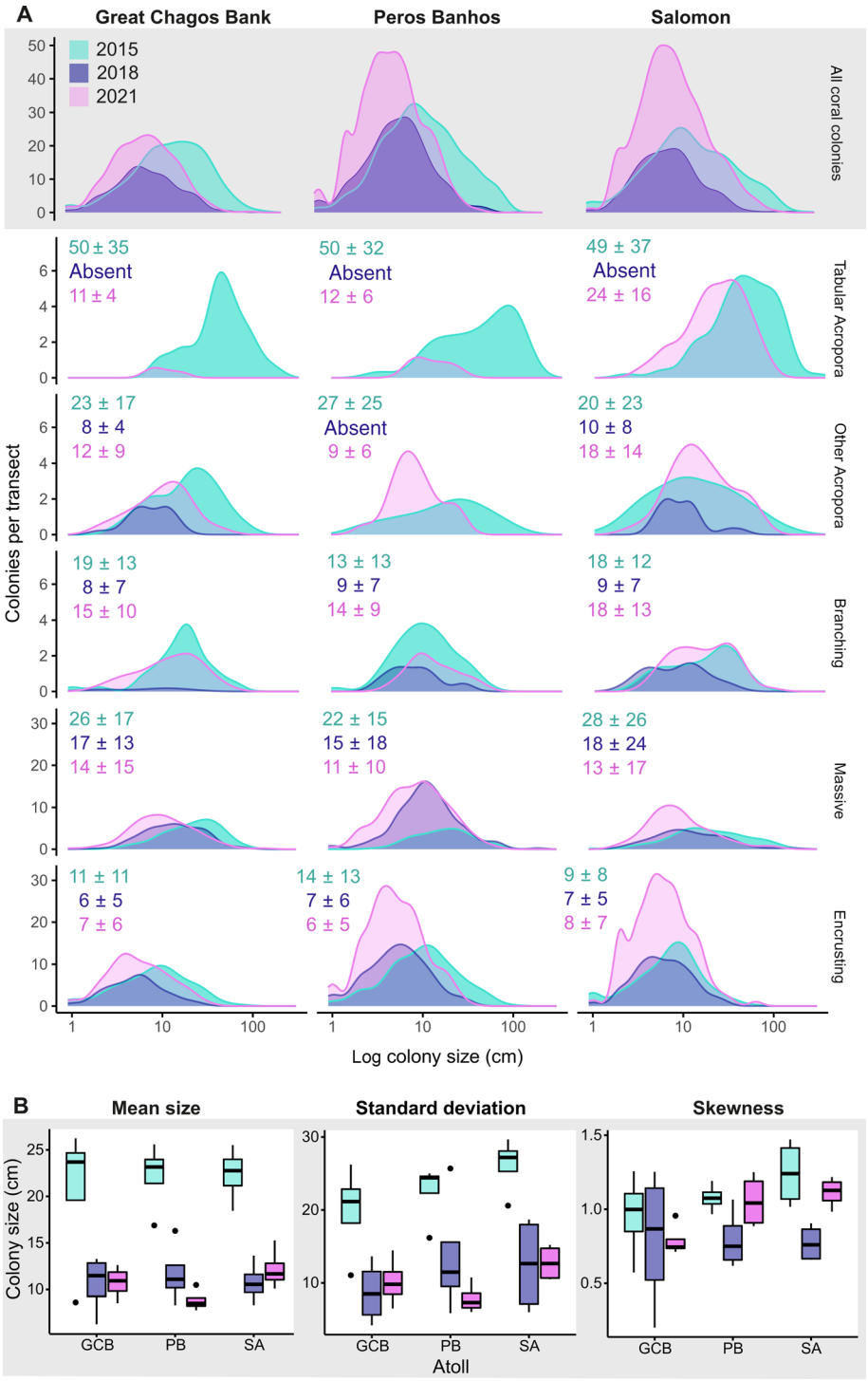

Fig. 3. Changes in coral population structure in response to the 2015/2016 bleaching event. (**A**) Size-frequency distributions of all coral colonies (first row) and different morphotypes (following rows) in Great Chagos Bank (GCB), Peros Banhos (PB), and Salomon atoll (SA) over time (color). Colony sizes are displayed on a log-scale and frequencies were calculated by dividing total frequencies in each atoll by the number of transects ($n = 16$/atoll). Note differences in *y*-axis scales comparing tabular/branching and massive/encrusting corals. Numbers in morphotype plots describe average size of colonies in each year in cm (mean ± SD); (**B**) site-level mean colony size, standard deviation and skewness of size distributions over all coral colonies at each atoll (x-axis) and over time (color). Boxplots represent median and inter-quartile range, with whiskers and points indicating minimum and maximum values.

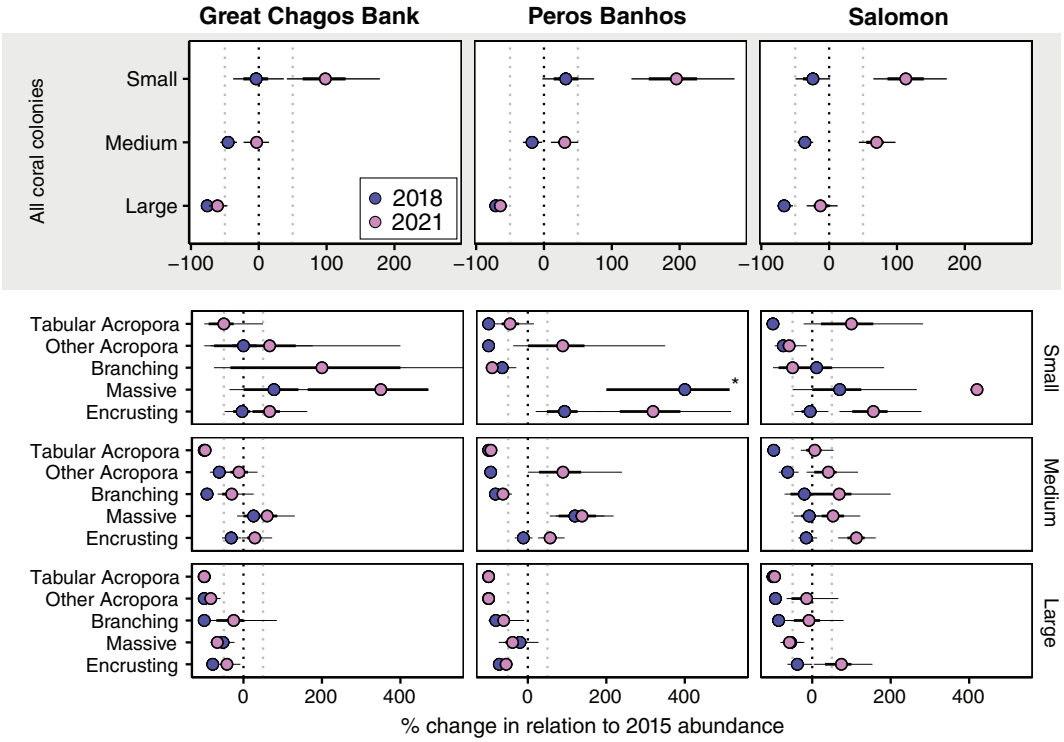

Fig. 4. Changes in coral colony abundance in response to the 2015/2016 bleaching event. Abundance of coral colonies in relation to 2015 values (mean ± 95%CI) for all colonies (first row) and different morphotypes (following rows) separated into different size classes (small: Within first quantile of morphotype-specific frequency distribution, medium: second to fourth quantile, large: fifth quantile). Vertical dashed lines indicate 0% (black) and 50% (gray) change in abundance compared to 2015 values. *The data point for small massive at Peros Banhos in 2021 is out of range (mean increase compared to 2015: 955%, 95% CI range: 371–2025%).

although these have yet to reach pre-bleaching sizes (Fig. 3A). Nevertheless, due to fast growth of branching and encrusting corals at Salomon, large colonies reached 87% of pre-bleaching abundances in 2021, while remaining at 36% and 39% of 2015 levels at Peros Banhos and Great Chagos Bank, respectively (Fig. 4).

Carbonate production, erosion, and net budget states

Changes in coral cover, community composition, and colony size distributions caused significant changes in reef carbonate budget metrics over time (Fig. 5A, Table 1). Average gross carbonate production dropped from 7.5 ± 2.2 G in 2015 to 2.4 ± 0.8 G in 2018 (23–37% of pre-bleaching values) but recovered to 4.1 ± 1.6 G by 2021 (36%, 45%, and 81% of pre-bleaching values at GCB, PB, and SA, respectively) (ANOVA, *year*: $F = 41.65$, $p < 0.001$; Supplementary Table S1). Averaged across all years, reefs in Salomon and Peros Banhos produced more carbonate than reefs in Great Chagos Bank (ANOVA, *atoll*: $F = 5.05$, $p = 0.014$; Supplementary Table S1). More interestingly, however, gross production rates in 2021 were much higher at Salomon compared to both other atolls (Table 1, Fig. 5A), despite similar live coral cover across sites (Fig. 2). As reefs in Salomon retained a higher structural complexity of underlying reef framework, that is, more reef surface per unit area, this may be caused by higher absolute coral area per planar reef area. Absolute coral cover can be calculated from actual measured coral tissue in each linear transect meter and indeed showed much higher values at Salomon (55 ± 5 cm^2 m^{-1}) compared to Peros Banhos (38 ± 7 cm^2 m^{-1}) and Great Chagos Bank (24 ± 9 cm^2 m^{-1}) in 2021. Additionally, the higher relative cover of fast-growing *Acropora* spp. at Salomon atoll facilitated higher carbonate production rates per live tissue area compared to other atolls.

Differences in gross erosion were not significant over time (2015: −3.8 ± 1.7 G, 2018: −4.8 ± 1.1 G, 2021: −4.4 ± 1.4 G), but significantly lower at Salomon (−3.4 ± 1.3G) compared to other atolls (GCB: −4.8 ± 1.0 G, PB: −4.8 ± 1.6 G) (ANOVA, *atoll*: $F = 5.30$, $p = 0.011$; Supplementary Table S1). The spatial difference in erosion was especially evident in 2015 and reflected lower parrotfish biomass at Salomon (Fig. 5B), which however was not caused by lower abundances but by smaller mean size of parrotfish (GCB: 46 ± 13 cm, PB: 39 ± 10 cm, SA: 22 ± 9 cm; Kruskal–Wallis all years: $\chi^2 = 16.88$, $p < 0.001$; Supplementary Table S3). Salomon was the only atoll that saw an increase in parrotfish abundance and biomass from 2015 to 2018 (Fig. 5B), which led to an increase in parrotfish bioerosion rates (Table 1). At Peros Banhos and Great Chagos Bank, parrotfish biomass in contrast decreased slightly due to

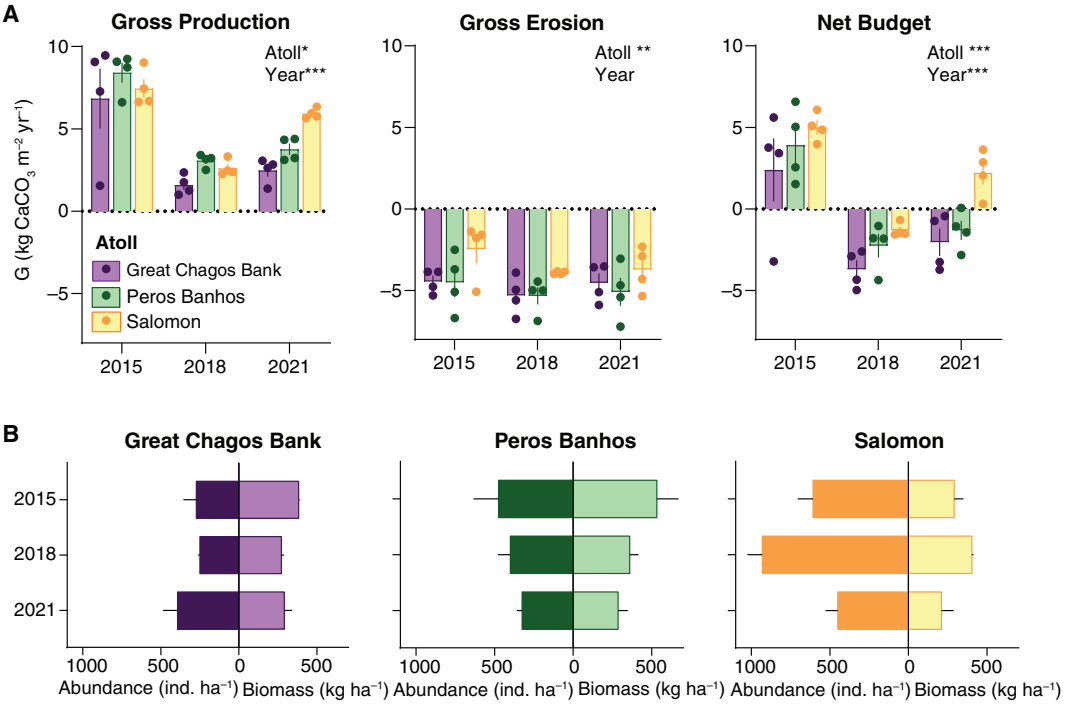

Fig. 5. Changes in carbonate budget states across the Chagos Archipelago in response to the 2015/2016 bleaching event. (**A**) Gross carbonate production, gross carbonate erosion, and net carbonate budgets in each atoll (color) over time (*x*-axis). Points represent site-level data and bar plots indicate mean ± SE at each atoll. Results from two-way ANOVAs are indicated by significance levels in the upper right corner (*< 0.05, **< 0.01, ***< 0.001), full ANOVA tables with Tukey post-hoc results are provided in Table S1. (**B**) Parrotfish abundance (left *x*-axis) and biomass (right *x*-axis) at each atoll (color) over time (*y*-axis). Bars and whiskers indicate mean + SE.

a decrease in mean fish size in 2018 (GCB: 36 ± 10 cm, PB: 32 ± 9 cm, SA: 25 ± 10 cm) and 2021 (GCB: 29 ± 12 cm, PB: 31 ± 14 cm, SA: 24 ± 12 cm). Other bioeroding species had much lower impacts on total gross bioerosion, although sea urchin erosion contributed substantially in Great Chagos Bank (up to −1.6 ± 1.2 G, Table 1), where three reef sites were continually exposed to erosion by very large *Diadema* spp. (test sizes 4–16 cm), which were never observed at any other site. However, gross erosion rates in 2021 were very similar across all atolls (Fig. 5A). Changes in net budgets over time and differences between atolls in 2021 are therefore primarily a function of carbonate production changes.

While net carbonate budgets did not differ across the atolls pre-bleaching (Fig. 5A), net budgets changed significantly over time (2015: 3.8 ± 2.6 G, 2018: −2.4 ± 1.4 G, 2021: −0.4 ± 2.3 G) (ANOVA: $F = 34.93$, $p < 0.001$; Supplementary Table S1) and were overall higher at Salomon compared to the other two atolls (Table 1; ANOVA: $F = 8.48$, $p = 0.001$; Supplementary Table S1). This is especially obvious in 2021, with sites at Salomon recovering to positive net budget states (2.2 ± 1.4 G), while all other sites are still net eroding (GCB: −2.0 ± 1.7 G, PB: −1.3 ± 1.2 G).

Discussion

Our results show extensive impacts of the 2015/2016 bleaching event on community composition, coral colony size distributions and reef carbonate budgets across fore reefs in the remote Chagos Archipelago. Five to six years after large-scale coral mortality, recovery is evident at all sites, but magnitude and trajectories differ between atolls. Fastest recovery is occurring at sites that retained higher framework structural complexity and experienced higher recruitment of tabular *Acropora* spp., illustrating the important role of this taxon for overall coral cover, structural complexity, and carbonate budgets. The observed trajectories are representative of naturally variable recovery patterns in reef systems undisturbed by local human impacts and can serve as a baseline to understand more anthropogenically impacted reefs across the Indo-Pacific.

Coral community changes

The magnitude of bleaching-driven changes in coral cover and community composition in the Chagos Archipelago was similar to that found on other reefs in the Indian Ocean, which experienced major losses of *Acropora* spp. and branching corals and a shift in dominance towards massive and encrusting taxa after the 1997/1998 and 2015/2016 bleaching events (McClanahan et al. 2007; Perry and Morgan 2017; Sheppard et al. 2017). The coral cover recovery rates observed in our study over the following years (mean ± SD: 3.1 ± 1.6% yr^{-1}) are also comparable to global averages after previous bleaching events (3.1 ± 1.6% yr^{-1}, Graham

et al. (2011)). Relatively slow early recovery usually reflects low initial recruitment levels in isolated coral communities and the dominance of unstable substrate for settlement, while recently dead coral skeletons denude (Gilmour et al. 2013). Indeed, juvenile coral densities across the Chagos Archipelago were found to be low from 2017 to 2019 (Sheppard et al. 2020) and reefs in 2018 and were characterized by high cover of rubble and dead *Acropora* tables. However, by 2021 the abundance of juvenile corals was high and it may be reasonable to predict that recovery is likely to speed up after the initial post-bleaching years as was observed at many sites across the Indian Ocean region after the 1997/1998 bleaching event (Graham et al. 2015; Morri et al. 2015; Sheppard et al. 2017). Even if calcification and recruitment rates are maintained at current levels, the ongoing recovery trajectories toward pre-bleaching communities reported here provide grounds for optimism that full recoveries of reef states and functions may occur within a similar time frame observed after the 1997/1998 bleaching event (7–15 yr depending on descriptor [coral cover, community composition, etc.]) (Gilmour et al. 2013; Morri et al. 2015; Sheppard et al. 2017). Nevertheless, concerns remain that some species and communities across the Chagos Archipelago may have gone functionally extinct and may not return to pre-bleaching states (Sheppard et al. 2020), the consequences of which will require on-going monitoring.

For a realistic assessment of recovery trajectories, it is therefore important to look at reef health indicators beyond coral cover. Size-frequency distributions of coral populations provide useful information on the responses of populations to environmental change (Meesters et al. 2001; McClanahan et al. 2008; Dietzel et al. 2020). The disappearance of large colonies alongside a relative increase in small colonies in our study supports findings of reduced mean colony size and higher relative abundances of small colonies in the Red Sea (Riegl et al. 2012) and in Kenya (McClanahan et al. 2008) 8–10 yr after the 1997/1998 bleaching. In contrast, a disproportionate loss of small colonies was observed at degraded reefs in the Southern Caribbean and the Great Barrier Reef (Meesters et al. 2001; Dietzel et al. 2020), indicating deficiencies in coral recruitment after mortality of the brood stock (Bak and Meesters 1998; Hughes and Tanner 2000). These contrasting demographic findings may be partly due to methodological differences, as both Meesters et al. (2001) and Dietzel et al. (2020) estimated the size of whole coral colonies including live and dead tissue, whereas our study and that of McClanahan et al. (2008) defined a colony as area of continuous live tissue, which means small colony sizes can also result from tissue fragmentation of larger colonies through partial mortality. In our study, this may be the case for massive and encrusting morphotypes, where high abundances of small colonies in 2018 likely reflect partial mortality of medium-sized and large colonies. However, over the following 3 yr, abundances in the small colony size class increased while numbers of medium and large-sized colonies remained stable or increased, indicating that these taxa are indeed recruiting successfully after 2018. High local recruitment levels are even more obvious for tabular *Acropora* spp. at Salomon, and for other *Acropora* spp. and branching corals at all atolls, as colony abundances of these taxa increased rapidly from 2018 to 2021 across small and medium size classes. This means that reproduction and larval recruitment is increasingly taking place and survival of juveniles appears high. Similarly, high recruitment levels were found in the remote Aldabra Atoll by 2019, with abundances of coral recruits and juveniles exceeding pre-bleaching numbers (Koester et al. 2021). Another difference to consider when comparing size-frequency studies is time after disturbance, as Dietzel et al. (2020) evaluated changes in communities directly after back-to-back bleaching events without time for new recruitment. An evaluation over a longer time frame and including several observations over time is however necessary to draw meaningful conclusions on reef health and recovery. While it is a growing and justified concern that disturbance intervals are becoming too short to allow the recovery of population size structures (Graham et al. 2011), the recovery of medium- and large-sized colonies only 6 yr after bleaching as reported in this study is indicative of strong recovery potential for reefs in the Chagos Archipelago. In contrast, reefs in Kenya and the Red Sea seemed to be locked into alternate community size structures even 10 yr after the 1997/1998 bleaching event (McClanahan et al. 2008; Riegl et al. 2012).

Recovery of reef functions

Shifts in community composition and coral colony size structure can have cascading effects on ecosystem functioning, as large colonies often contribute disproportionally more to structural complexity and reproduction (Alvarez-Filip et al. 2011), while small colonies can disproportionally increase carbonate production in the short-term (Carlot et al. 2021). This also means that spatial differences in community structure may strongly determine recovery trajectories of reefs. However, contrary to Carlot et al. (2021), who highlight the importance of juvenile colonies to bolster carbonate budgets after bleaching events, our study shows a surprisingly close accordance of coral carbonate production recovery toward pre-bleaching levels (return to 85%, 46%, and 37% of 2015 carbonate production rates at SA, PB, and GCB, respectively) with the abundance of coral colonies in large-size classes in 2021 (SA: 87%, PB: 36%, GCB: 39% of 2015 values). Size-specific differences in calcification rates were not obtained in our study and the increase in numbers of large colonies might simply lead to increased coral cover and consequently carbonate production. However, total live coral reached similar coverages in all atolls in 2021, but the much higher values of carbonate production at Salomon suggest that relative cover of live coral on its own is not a good indicator of reef health and functions. Similarly, previous studies have emphasized

that coral cover should not be used as the only predictor of carbonate budget status or reef functionality, especially when communities shift away from mayor framework builders, as evident in the Caribbean (Perry et al. 2015*b*; González-Barrios et al. 2021).

In this context, we show that in addition to coral cover, reef structural complexity and the abundance of key functional species (fast-growing tabular *Acropora* in this case) appear key predictors of carbonate budget recovery in the Chagos Archipelago. The maintenance of structural complexity is a known crucial factor for reef resilience, as a diverse habitat provides shelter and feeding ground for herbivorous fish (Graham et al. 2007) and presents suitable topographical features for coral settlement (Connell et al. 1997). As mentioned in the results section, high reef rugosity can also increase absolute coral cover per planar reef area by providing multiple levels of substrate. This means that reefs that have and maintain a high structural complexity and associated reef functions appear capable of more rapid recovery from large-scale disturbances. Indeed, time scales of ecological recovery have been shown to vary depending on the physical structure that was left in place (Tanner 2017). Differences in reef structure complexity after disturbance may be caused by variability in wave exposure, which can affect the rate at which new coral habitat is formed and reef structure degrades (Madin et al. 2016). The differences in recovery rates between atolls in our study may therefore partly be explained by differences in wave exposure among study sites, as the west shore of Salomon is more protected from long distance southern swells and westerly winds that those of Peros Banhos and Great Chagos Bank due to the orientation of the atoll (Fig. 1). Although the dominant wind direction is from the southeast with maximum wind speeds from June to September, occasional strong westerly winds are likely. Indeed, faster coral recovery has been observed during exploration dives at north-facing, potentially more sheltered reef sites in Peros Banhos in 2021 (ID Lange, pers. obs.). However, Lange et al. (2021) showed that fast recovery of *Acropora* spp. is taking place around the entire Salomon atoll despite large gradients in wave exposure, suggesting that availability of brood stock and larvae might be equally important as differences in exposure at the inter-atoll scale.

High reef connectivity and coral recruitment are critical for reef recovery and are especially important for remote, isolated areas (Ayre and Hughes 2004; Jones et al. 2009; Edmunds et al. 2018). For instance, spatial differences in recovery around Mo'orea were independent of structural complexity and driven almost entirely by larval supply (Holbrook et al. 2018). Coral recruitment was not directly quantified in this study, but higher success at Salomon compared to other atolls was indicated by the increased abundance of small coral colonies in 2021, critically including many tabular *Acropora* spp., and a higher positive skewness of size distributions (i.e., relatively more small colonies). Larval supply at Salomon's fore reefs was most likely enhanced by the proximity to healthy coral populations within the shallow, semi-closed lagoon, which suffered little mortality during the 2015/2016 bleaching event, probably due to local adaptation to high water temperatures (Benkwitt et al. 2019). There are indications that connectivity and juvenile density are main drivers of recovery of fast-growing *Acropora*, but not for other groups (Gouezo et al. 2019), which is somewhat supported by our study that shows largest inter-atoll differences in the numbers of tabular *Acropora* and branching corals. Connectivity depends on small-scale oceanographic processes, which can not only deliver coral larvae but also particle-rich lagoonal waters to the shallow outer reef terrace (Williams et al. 2018). As heterotrophy can increase persistence of corals under harsh environmental conditions (Anthony 2006; Borell et al. 2008) and their recovery following disturbance (Grottoli et al. 2006; Connolly et al. 2012; Levas et al. 2016), particle-rich lagoonal waters serving as additional food source for Salomon's outer reefs may also play a role for divergent trajectories of recovery and should be investigated in more detail.

Besides structural complexity and coral recruitment, high levels of herbivory are known to increase recovery potential of reefs (Mumby et al. 2007; Burkepile and Hay 2008; Adam et al. 2011). Changes in parrotfish demographics following bleaching have been observed in the southern Maldives (Perry et al. 2020) and other areas (e.g., Adam et al. 2011; Gilmour et al. 2013; Russ et al. 2015) and are associated with a positive growth response following increased food availability after wide-spread coral mortality (Taylor et al. 2020). An increase in size and density of parrotfish in turn leads to increased rates of grazing and bioerosion, which has been suggested to facilitate coral recruitment (Burkepile and Hay 2008; Cramer et al. 2017). Fish surveys in this study indicated a positive signal in abundance and biomass of parrotfish after the 2015/2016 bleaching event at Salomon atoll, but not in Peros Banhos or the Great Chagos Bank. A reason for this difference could be the sustained structural complexity on Salomon's reefs, which offers a more diverse feeding ground and shelter for larger fish. Although the observed increase in bioerosion at Salomon atoll after the bleaching was rather small ($1.5\ kg\ m^{-2}\ yr^{-1}$), it may represent an additional factor contributing to the faster recovery of reefs in this atoll compared to Peros Banhos and Great Chagos Bank.

Summary

Fore reefs across the remote Chagos Archipelago are on a trajectory of recovery after the 2015/2016 bleaching event, but the speed varies considerably across atolls and affects resultant reef geo-ecological functions. At Salomon atoll, the maintenance of high framework structural complexity and rapid recovery of tabular *Acropora* spp. has underpinned a return to net positive carbonate budgets within only 6 yr post-bleaching, while sites at other atolls are recovering more slowly. Inter-atoll differences in colony size distributions

illustrate the important role that branching and tabular *Acropora* spp. play for the recovery of structural complexity and reef carbonate budgets. It is also evident that higher abundances of small colonies do not outweigh the loss of large colonies in terms of carbonate production, and that live coral cover alone is not an accurate predictor of reef functions. For more in-depth analysis of the drivers of intra- and inter-atoll differences in recovery trajectories, the collection of detailed environmental data will be necessary to complement the presented ecological datasets. Although reefs in Great Chagos Bank and Peros Banhos were still net eroding in 2021, reasonably fast recovery of coral cover and carbonate budgets was evident across all sites and suggests potential for full recovery of associated reef functions within the next few years. The return to pre-bleaching levels of structural complexity and reef growth may however be impacted by recurrent bleaching events in the near future. The observed patterns are representative of natural recovery trajectories in reef systems undisturbed by local human impacts, a deeper understanding of which is urgently needed to predict ecosystem trajectories and manage reefs under increasing global threats.

Data availability

All data can be downloaded from the University of Exeter Open Research Repository at https://doi.org/10.24378/exe.3863.

References

Adam, T. C., R. J. Schmitt, S. J. Holbrook, A. J. Brooks, P. J. Edmunds, R. C. Carpenter, and G. Bernardi. 2011. Herbivory, connectivity, and ecosystem resilience: Response of a coral reef to a large-scale perturbation. PLoS one **6**: e23717.

Alvarez-Filip, L., N. K. Dulvy, I. M. Côté, A. R. Watkinson, and J. A. Gill. 2011. Coral identity underpins architectural complexity on Caribbean reefs. Ecol. Appl. **21**: 2223–2231.

Anderson, M. J. 2005. Permutational multivariate analysis of variance, v. **26**. Department of Statistics, University of Auckland, p. 32–46.

Anderson, M. J., and D. C. Walsh. 2013. PERMANOVA, ANOSIM, and the Mantel test in the face of heterogeneous dispersions: What null hypothesis are you testing? Ecol Monogr **83**: 557–574.

Anthony, K. R. 2006. Enhanced energy status of corals on coastal, high-turbidity reefs. Mar. Ecol. Prog. Ser. **319**: 111–116.

Ayre, D. J., and T. P. Hughes. 2004. Climate change, genotypic diversity and gene flow in reef-building corals. Ecol. Lett. **7**: 273–278.

Bak, R. 1994. Sea urchin bioerosion on coral reefs: Place in the carbonate budget and relevant variables. Coral Reefs **13**: 99–103.

Bak, R. P., and E. H. Meesters. 1998. Coral population structure: The hidden information of colony size-frequency distributions. Mar. Ecol. Prog. Ser. **162**: 301–306.

Bellwood, D. R. 1995. Direct estimate of bioerosion by two parrotfish species, Chlorurus gibbus and C. sordidus, on the Great Barrier Reef, Australia. Mar Biol **121**: 419–429.

Bellwood, D. R., and J. H. Choat. 1990. A functional analysis of grazing in parrotfishes (family scaridae) - the ecological implications. Environ. Biol. Fishes **28**: 189–214.

Benkwitt, C. E., S. K. Wilson, and N. A. Graham. 2019. Seabird nutrient subsidies alter patterns of algal abundance and fish biomass on coral reefs following a bleaching event. Glob. Chang. Biol. **25**: 2619–2632.

Borell, E. M., A. R. Yuliantri, K. Bischof, and C. Richter. 2008. The effect of heterotrophy on photosynthesis and tissue composition of two scleractinian corals under elevated temperature. J. Exp. Mar. Biol. Ecol. **364**: 116–123.

Brandl, S. J., D. B. Rasher, I. M. Côté, J. M. Casey, E. S. Darling, J. S. Lefcheck, and J. E. Duffy. 2019. Coral reef ecosystem functioning: Eight core processes and the role of biodiversity. Front. Ecol. Environ. **17**: 445–454.

Bruggemann, J. H., A. M. van Kessel, J. M. van Rooij, and A. M. Breeman. 1996. Bioerosion and sediment ingestion by the Caribbean parrotfish Scarus vetula and Sparisoma viride: Implications of fish size, feeding mode and habitat use. Mar. Ecol. Prog. Ser. **134**: 59–71.

Bucher, D. J., V. J. Harriott, and L. G. Roberts. 1998. Skeletal micro-density, porosity and bulk density of acroporid corals. J. Exp. Mar. Biol. Ecol. **228**: 117–136.

Burkepile, D. E., and M. E. Hay. 2008. Herbivore species richness and feeding complementarity affect community structure and function on a coral reef. Proc. Natl. Acad. Sci. **105**: 16201–16206.

Carlot, J., and others. 2021. Juvenile corals underpin coral reef carbonate production after disturbance. Glob. Chang. Biol. **27**: 2623–2632.

Clarke, K. R. 1993. Non-parametric multivariate analyses of changes in community structure. Austr J Ecol **18**: 117–143.

Connell, J. H., T. P. Hughes, and C. C. Wallace. 1997. A 30-year study of coral abundance, recruitment, and disturbance at several scales in space and time. Ecol Monogr **67**: 461–488.

Connolly, S. R., M. Lopez-Yglesias, and K. R. Anthony. 2012. Food availability promotes rapid recovery from thermal stress in a scleractinian coral. Coral Reefs **31**: 951–960.

Cramer, K. L., A. O'Dea, T. R. Clark, J. X. Zhao, and R. D. Norris. 2017. Prehistorical and historical declines in Caribbean coral reef accretion rates driven by loss of parrotfish. Nat. Commun. **8**: 14160.

Dietzel, A., M. Bode, S. R. Connolly, and T. P. Hughes. 2020. Long-term shifts in the colony size structure of coral populations along the Great Barrier Reef. Proc. R. Soc. B **287**: 20201432.

Edmunds, P. J., and others. 2018. Critical information gaps impeding understanding of the role of larval connectivity among coral reef islands in an era of global change. Front. Mar. Sci. **5**: 290.

Edmunds, P. J., C. Didden, and K. Frank. 2021. Over three decades, a classic winner starts to lose in a Caribbean coral community. Ecosphere **12**: e03517.

Gilmour, J. P., L. D. Smith, A. J. Heyward, A. H. Baird, and M. S. Pratchett. 2013. Recovery of an isolated coral reef system following severe disturbance. Science **340**: 69–71.

González-Barrios, F. J., R. A. Cabral-Tena, and L. Alvarez-Filip. 2021. Recovery disparity between coral cover and the physical functionality of reefs with impaired coral assemblages. Glob. Chang. Biol. **27**: 640–651.

Gouezo, M., Y. Golbuu, K. Fabricius, D. Olsudong, G. Mereb, V. Nestor, E. Wolanski, P. Harrison, and C. Doropoulos. 2019. Drivers of recovery and reassembly of coral reef communities. Proc. R. Soc. B **286**: 20182908.

Graham, N. A., S. K. Wilson, S. Jennings, N. V. Polunin, J. Robinson, J. P. Bijoux, and T. M. Daw. 2007. Lag effects in the impacts of mass coral bleaching on coral reef fish, fisheries, and ecosystems. Conserv. Biol. **21**: 1291–1300.

Graham, N., K. Nash, and J. Kool. 2011. Coral reef recovery dynamics in a changing world. Coral Reefs **30**: 283–294.

Graham, N. A. J., S. Jennings, M. A. MacNeil, D. Mouillot, and S. K. Wilson. 2015. Predicting climate-driven regime shifts versus rebound potential in coral reefs. Nature **518**: 94–97.

Grottoli, A. G., L. J. Rodrigues, and J. E. Palardy. 2006. Heterotrophic plasticity and resilience in bleached corals. Nature **440**: 1186–1189.

Hays, G. C., and others. 2020. A review of a decade of lessons from one of the world's largest MPAs: Conservation gains and key challenges. Mar. Biol. **167**: 159.

Hodgson, D., J. L. McDonald, and D. J. Hosken. 2015. What do you mean,'resilient'? Trends Ecol. Evol. **30**: 503–506.

Holbrook, S. J., T. C. Adam, P. J. Edmunds, R. J. Schmitt, R. C. Carpenter, A. J. Brooks, H. S. Lenihan, and C. J. Briggs. 2018. Recruitment drives spatial variation in recovery rates of resilient coral reefs. Sci Rep **8**: 1–11.

Hughes, T. P., and J. E. Tanner. 2000. Recruitment failure, life histories, and long-term decline of Caribbean corals. Ecology **81**: 2250–2263.

Jones, G., G. Almany, G. Russ, P. Sale, R. Steneck, M. Van Oppen, and B. Willis. 2009. Larval retention and connectivity among populations of corals and reef fishes: History, advances and challenges. Coral Reefs **28**: 307–325.

Koester, A., A. K. Ford, S. C. A. Ferse, V. Migani, N. Bunbury, C. Sanchez, and C. Wild. 2021. First insights into coral recruit and juvenile abundances at remote Aldabra Atoll, Seychelles. PLos One **16**: e0260516.

Lange, I. D., and C. T. Perry. 2019. Bleaching impacts on carbonate production in the Chagos archipelago: Influence of functional coral groups on carbonate budget trajectories. Coral Reefs **38**: 619–624.

Lange, I. D., and C. T. Perry. 2020. A quick, easy and non-invasive method to quantify coral growth rates using photogrammetry and 3D model comparisons. Methods Ecol Evol **11**: 714–726.

Lange, I. D., C. T. Perry, K. M. Morgan, R. Roche, C. E. Benkwitt, and N. A. Graham. 2020. Site-level variation in parrotfish grazing and bioerosion as a function of species-specific feeding metrics. Diversity **12**: 379.

Lange, I. D., and others. 2021. Wave exposure shapes reef community composition and recovery trajectories at a remote coral atoll. Coral Reefs **40**: 1819–1829.

Leupold, M., M. Pfeiffer, D. Garbe-Schönberg, and C. Sheppard. 2019. Reef-scale-dependent response of massive Porites corals from the Central Indian Ocean to prolonged thermal stress: Evidence from coral Sr/Ca measurements. Geochem. Geophys. Geosyst. **20**: 1468–1484.

Levas, S., A. G. Grottoli, V. Schoepf, M. Aschaffenburg, J. Baumann, J. E. Bauer, and M. E. Warner. 2016. Can heterotrophic uptake of dissolved organic carbon and zooplankton mitigate carbon budget deficits in annually bleached corals? Coral Reefs **35**: 495–506.

Mace, G. M., and others. 2014. Approaches to defining a planetary boundary for biodiversity. Glob. Environ. Chang. **28**: 289–297.

Madin, J. S., and others. 2016. A trait-based approach to advance coral reef science. Trends Ecol. Evol. **31**: 419–428.

Manzello, D. P., I. C. Enochs, G. Kolodziej, R. Carlton, and L. Valentino. 2018. Resilience in carbonate production despite three coral bleaching events in 5 years on an inshore patch reef in the Florida Keys. Mar. Biol. **165**: 99.

McClanahan, T., M. Ateweberhan, N. Graham, S. Wilson, C. R. Sebastián, M. M. Guillaume, and J. H. Bruggemann. 2007. Western Indian Ocean coral communities: Bleaching responses and susceptibility to extinction. Mar. Ecol. Prog. Ser. **337**: 1–13.

McClanahan, T., M. Ateweberhan, and J. Omukoto. 2008. Long-term changes in coral colony size distributions on Kenyan reefs under different management regimes and across the 1998 bleaching event. Mar. Biol. **153**: 755–768.

Meesters, E., M. Hilterman, E. Kardinaal, M. Keetman, M. DeVries, and R. Bak. 2001. Colony size-frequency distributions of scleractinian coral populations: Spatial and interspecific variation. Mar. Ecol. Prog. Ser. **209**: 43–54.

Molina-Hernández, A., F. J. González-Barrios, C. T. Perry, and L. Álvarez-Filip. 2020. Two decades of carbonate budget change on shifted coral reef assemblages: Are these reefs being locked into low net budget states? Proc. R. Soc. B **287**: 20202305.

Morgan, K. M., and P. S. Kench. 2014. Carbonate production rates of encruster communities on a lagoonal patch reef: Vabbinfaru reef platform, Maldives. Mar Freshw Res **65**: 720.

Morri, C., M. Montefalcone, R. Lasagna, G. Gatti, A. Rovere, V. Parravicini, G. Baldelli, P. Colantoni, and C. N. Bianchi. 2015. Through bleaching and tsunami: Coral reef recovery in the Maldives. Mar. Pollut. Bull. **98**: 188–200.

Mumby, P. J., A. Hastings, and H. J. Edwards. 2007. Thresholds and the resilience of Caribbean coral reefs. Nature **450**: 98–101.

Oksanen J, and others. 2020. vegan: Community Ecology Package. R package version 25-7.

Perry, C. T., T. Spencer, and P. Kench. 2008. Carbonate budgets and reef production states: A geomorphic perspective on the ecological phase-shift concept. Coral Reefs **27**: 853–866.

Perry, C. T., G. N. Murphy, N. A. Graham, S. K. Wilson, F. A. Januchowski-Hartley, and H. K. East. 2015*a*. Remote coral reefs can sustain high growth potential and may match future sea-level trends. Sci Rep **5**: 18289.

Perry, C. T., R. S. Steneck, G. N. Murphy, P. S. Kench, E. N. Edinger, S. G. Smithers, and P. J. Mumby. 2015*b*. Regional-scale dominance of non-framework building corals on Caribbean reefs affects carbonate production and future reef growth. Glob. Chang. Biol. **21**: 1153–1164.

Perry, C. T., and K. M. Morgan. 2017. Bleaching drives collapse in reef carbonate budgets and reef growth potential on southern Maldives reefs. Sci Rep **7**: 40581.

Perry, C. T., and others. 2018. Loss of coral reef growth capacity to track future increases in sea level. Nature **558**: 396–400.

Perry, C. T., K. M. Morgan, I. D. Lange, and R. T. Yarlett. 2020. Bleaching-driven reef community shifts drive pulses of increased reef sediment generation. R. Soc. Open Sci. **7**: 192153.

Pratchett, M., C. Thompson, A. Hoey, P. Cowman, and S. Wilson. 2018. Effects of coral bleaching and coral loss on the structure and function of reef fish assemblages coral bleaching. Springer, p. 265–293.

R Core Team. 2021. R: A language and environment for statistical computing. R Foundation for Statistical Computing.

Riegl, B. M., A. W. Bruckner, G. P. Rowlands, S. J. Purkis, and P. Renaud. 2012. Red Sea coral reef trajectories over 2 decades suggest increasing community homogenization and decline in coral size. PLoS One **7**: e38396.

Risk, M. J. 1972. Intertidal substrate rugosity and species diversity. Univ. of Southern California.

Russ, G. R., S.-L. A. Questel, J. R. Rizzari, and A. C. Alcala. 2015. The parrotfish–coral relationship: Refuting the ubiquity of a prevailing paradigm. Mar. Biol. **162**: 2029–2045.

Scoffin, T. 1993. The geological effects of hurricanes on coral reefs and the interpretation of storm deposits. Coral Reefs **12**: 203–221.

Sheppard, C. 2009. Large temperature plunges recorded by data loggers at different depths on an Indian Ocean atoll: Comparison with satellite data and relevance to coral refuges. Coral Reefs **28**: 399–403.

Sheppard, C. R. C., A. Sheppard, A. Mogg, D. Bayley, A. C. Dempsey, R. Roche, J. Turner, and S. Purkins. 2017. Coral bleaching and mortality in the Chagos Archipelago. Atoll Res Bull **613**: 1–26.

Sheppard, C., A. Sheppard, and D. Fenner. 2020. Coral mass mortalities in the Chagos archipelago over 40 years: Regional species and assemblage extinctions and indications of positive feedbacks. Mar. Pollut. Bull. **154**: 111075.

Tanner, J. E. 2017. Multi-decadal analysis reveals contrasting patterns of resilience and decline in coral assemblages. Coral Reefs **36**: 1225–1233.

Taylor, B. M., C. E. Benkwitt, H. Choat, K. D. Clements, N. A. Graham, and M. G. Meekan. 2020. Synchronous biological feedbacks in parrotfishes associated with pantropical coral bleaching. Glob. Chang. Biol. **26**: 1285–1294.

Tribollet, A., and S. Golubic. 2005. Cross-shelf differences in the pattern and pace of bioerosion of experimental carbonate substrates exposed for 3 years on the northern Great Barrier Reef, Australia. Coral Reefs **24**: 422–434.

West, J. M., and R. V. Salm. 2003. Resistance and resilience to coral bleaching: Implications for coral reef conservation and management. Conserv. Biol. **17**: 956–967.

Wickham, H., and others. 2019. Welcome to the tidyverse. J Open Source Softw **4**: 1686.

Williams, G. J., and others. 2018. Biophysical drivers of coral trophic depth zonation. Mar. Biol. **165**: 60.

Wilson, S., and others. 2010. Crucial knowledge gaps in current understanding of climate change impacts on coral reef fishes. J. Exp. Biol. **213**: 894–900.

Acknowledgments

This research was funded by the Bertarelli Foundation as part of the Bertarelli Programme in Marine Science and was conducted under permit numbers 0004SE18 and 0002SE21. The authors thank the ZSL support team as well as the captains and crews of the research vessel for logistical help.

Conflict of interest

The authors have no conflict of interest to declare.

Submitted 06 October 2021
Revised 03 January 2022
Accepted 06 March 2022

Associate editor: Susanne Menden-Deuer